International Journal of Environmental Sciences
ISSN: 2229-7359
Vol. 11 No. 7s, 2025
https://www.theaspd.com/ijes.php

GI Bleeding Detection in WCE Images Using E-ORB and ME-DEEP CAPSNET

Dr S. Rathnamala[1], Aghila Rajagopal[2], M. Arunachalam[3] and V. Dhanasekaran[4]
[1]Associate Professor, Department of AI&DS, Sethu Institute of Technology
[2]Professor, Department of AI&DS, Kamaraj College of Engineering and Technology
[3]Professor, Sri Krishna College of Engineering and Technology
[4]Assistant Professor, Velammal College of Engineering and Technology

Abstract: *Wireless Capsule Endoscopy (WCE) is utilized in the detection of several anomalies like bleeding, ulcers, polyps, and tumors in the gastrointestinal (GI) tract. As a huge number of images are produced by WCE, the manual examination becomes much more tedious, time-consuming, and furthermore increasing the possibility of human errors. Therefore, a new automated scheme to detect bleeding region in WCE images by means of deep learning technique is proposed in this approach. Initially, the WCE input images are pre-processed by means of distribution linearization and linear filtering. An Adaptive dense U-Net based segmentation approach is employed for the segmentation of pre-processed image. The feature point extraction is dome using Enhanced Oriented fast and Rotated BRIEF (ORB) algorithm. The detection process and the classification of detected region as bleeding and non-bleeding region is carried by Multi- Enhanced Deep CapsNet classification model. The performance assessment is carried in terms of accuracy, sensitivity, specificity, precision, recall, F-measure, FNR, and FPR, and the outcomes acquired are compared with existing methods to validate the improvement of proposed scheme.*
Index Terms*—WCE, GI tract, Adaptive dense U-Net segmentation, ORB algorithm, Multi-Enhanced Deep CapsNet classifier.*

I. INTRODUCTION

Wireless Capsule Endoscope (WCE) is regarded as a technique which is utilized for assessing and visualizing the body parts of Gastrointestinal tract (GI) tract that are inaccessible mostly to doctors [1]. This part of bowel is not capable to reach by means of traditional methods like upper endoscopy and colonoscopy. An usual cause of such capsule endoscopy is for exploring the cause of bleeding in small intestine [2,3]. It is also utilized to recognize inflammatory bowl disease, ulcers, polyps at small intestine and tumours. Moreover, this WCE that are accessible commercially may partake several limitations like: low image quality, insufficient time of working, and lower rate of accuracy. The analysis and evaluation of entire recorded images from capsule by manual method is a tiresome and a time-consuming process [4]. Therefore, a computerized methods are focussed in various techniques that reduces the physician's burden which may result in decreased processing time.

Gastrointestinal tract bleeding is considered as a sign of dreadful digestive system. By the advancement of some medical imaging approaches, it could be utilized in a huge medical application range to detect and diagnosing purpose thereby interevent at time by means of several pathologists. Typically, WCE is considered as an indispensable process to treat and diagnose diseases and abnormalities of GI tract. By the discovery of WCE, it is proved to be an accepted technique for the visualization of GI tract images due to its clinical values and safety [5]. As the detection of bleeding in WCE images is a challenging aspect, the detection through computer aided process utilization aids in the detection of GI bleeding that results in formulation and solution of several patterns of recognition and a problem of classification.

Several machine and deep learning techniques have been employed so far to detect the bleeding and abnormalities of GI tract [6,7]. However, each technique is facing some challenges and there is a need

to develop some advancement in existing techniques to increase the accuracy and performance of detection mechanism. For this purpose, a deep learning-based scheme is employed in this work so as to recognize and classify the bleeding and non-bleeding regions of GI tract and to found any abnormalities present.

This manuscript is organized as shown: Section II is the short review made on various traditional methodologies employed in the detection of WCE images. The proposed technique is narrated in detail in section III. The assessment made to estimate the performance and enhancement of proposed method over existing method is illustrated in section IV. The concluding remark is provided in section V.

I. RELATED WORKS

A fully automated system to recognize the stomach deformities was suggested in [8] based on the deep learning feature selection and fusion. In this, ulcer images were manually designed to support the saliency-based method to detect ulcer. after that, the technique of pre-trained deep learning model termed VGG16 was employed and is re- trained using a transfer learning model.

Experiments were conducted collected dataset that were gathered privately and the outcome attained shows that it achieves an accuracy rate of about 98.4% which was enhanced on comparing existing methodologies.

In [9], WCE was widely employed and an automated technique was presented to diagnose the GI tract of patient to examine the internal walls of GI tract. However, there were still some limitations which limits the functionality on limiting their acceptance.

A technique of two stage image compression was suggested in [10] where the images of WCE are considered to offer images of good quality, higher compression rate with low computational complexity. The initial step employs a very low integer transform complexity that was then followed by effective Huffman coding and quantization method. Then, the rebuilt image was taken and post-processing is carried to attain high quality visual image.

An image based novel High level control system was presented in [11] that intends for real-time autonomous active capsule endoscope. In this method, at first a novel specific path was presented for the detection of stomach fold abnormality using an acquired input image. Then, various maneuvers are presented for following desired path which adjusts the orientation of capsule.

A deep learning-based abnormality identification in several endoscope techniques were estimated in (WCE, Gastroscopy, and colonoscopy) [12]. In the detection, domain segmentation, and classification, the deep learning models were presented as per the goal and intention of analyzing WCE image. The approaches that contribute the endoscopic image analysis were being addressed along with SegNet, AlexNet, LeNet, GoogleNet, VGGNet, ResNet, R-CNN, FCN, and DeepLab. A review was made by emphasizing the important fields of diagnosing deep learning system based on RNN, GNN, 3D- CNN, and a development of real-time video processing.

In [13], the author developed a computer aided model for the purpose of detection and diagnosis. Since, the erosions and ulcerations were the most common small bowel abnormalities found on WCE, a scheme of WCE was presented with the technique of deep learning model to detect erosions and ulcerations in an automatic manner from the WCE images. A scheme of deep CNN based on single shot multi-box detector using 5360 images of WCE erosion and ulcerations.

The author in [14] suggested a method to detect the WCE abnormal images in an automatic manner. The enumeration of differential box method was thus utilized for extraction of fractal images and a random forest-based ensemble classifier was presented. In this work, a fractal dimension was thus mined from the images of WCE pixel-block that are fed to classifier for the identification of image irregularities.

A method of RoI based segmentation that sinks the feature space complications in WCE images were considered. In the built areas, features unpredictability or else the RoI selection was intricate extremely. The process of region growing was frequently employed to examine the images of WCE in the bleeding region segmentation. A RoI was constructed from the seed region by this approach presented in [15] based on the statistics features considered from RG constructed RoI approach which acquires the region selection.

A technique with three stage was implemented in [16] to detect bleeding region based on super-pixel. The super-pixel histograms were thus employed for the classification of bleeding areas with the use of KNN. The leakage area was then differentiated over none space super-pixel colours. In the super-pixel based detection of ulcer technique, images of WCE were used.

A new review was analysed in [17] based on the evaluation offered on WCE based GI tract abnormalities detection technique which supports the need of united polyps, tumour collection system and ulcer detection.

The author in [18] presented a metric of vigorous comparation and a technique for adapting the super pixel integration. This technique presents comparison as a similarity mixture of the weighted content for the incorporation of smooth similarities of super pixel and boundaries. Based on the agglomeration base, super pixels were united.

In the work [19], a CAD system was presented for the automatic detection of ulcer from WCE images. The WCE has reformed the diagnosis and treatment of GI tract, specifically the small intestine that was inaccessible over traditional endoscopies. The drawback of WCE was that it provides a wide range of images that was being inspected through clinicians. From this, a system of CAD diagnosis that are having huge potential to support the reduction of time taken for diagnosis and thus increasing detection accuracy. To address these concerns, CAD system was presented to detect WCE ulcer images automatically.

A Deep Hookworm Detection (DHDF) Framework was developed in [20] that employs deep learning based WCE. Similarly, the context recommended duplicates the image look and a hookworm strategy that were like tube.

This too integrates two system of CNN that intends in the edge extraction and the hookworm classification for enhancing the process of classification by presented method.

II. PROPOSED WORK

The detail explanation on the proposed methodology workflow is narrated in this work. A depiction of overall working method flow is provided here.

International Journal of Environmental Sciences
ISSN: 2229-7359
Vol. 11 No. 7s, 2025
https://www.theaspd.com/ijes.php

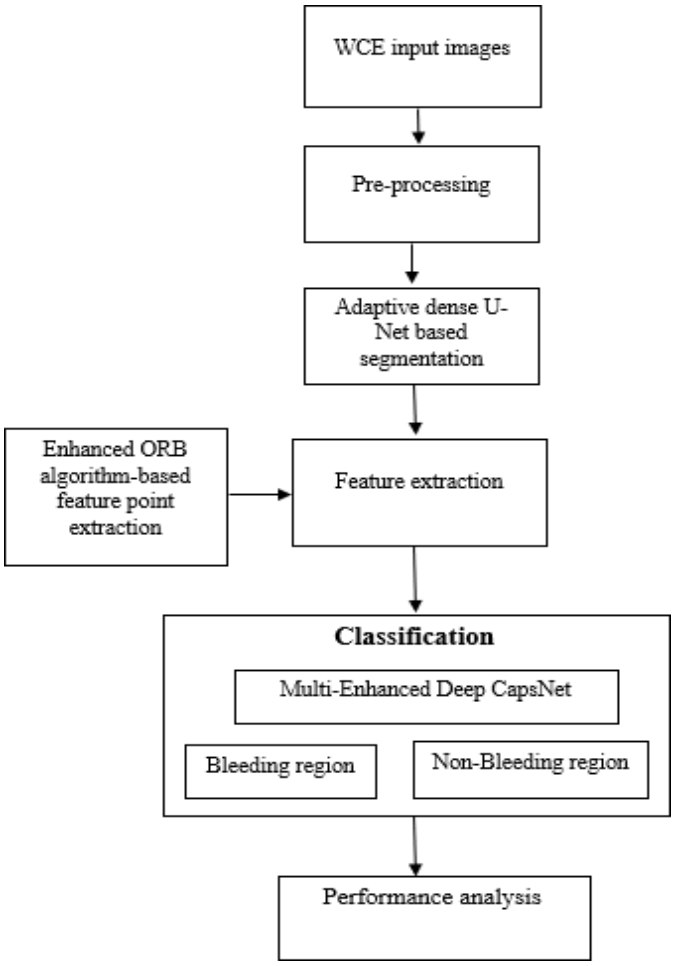

Figure 1 A representation of entire workflow of proposed technique

A. Pre-processing

The first phase includes noise generation followed by pre- processing with the use of distribution linearization and linear filtering approach. Before the extraction of feature and segmentation of image, this pre-processing is carried. The process of filtering is utilized in the pre-processing phase. The technique of distribution linearization is employed in grey level images so as to reduce noise, to attain fine quality information of image, and substituted data lack and intensity variance which decreases the quality thus altering the neighbourhood pixels. The noise reduction in GI images is considered as an effectual method. In this, median filter is tested for the reduction of noise. The method of distribution linearization is considered as a simple technique employed for the elimination of noise from the GI tract images. The determination of median value is carried by ordering the approved pixel and thereby moving the pixel consideration to the centre of pixel ranking. The difference among the pixel is calculated by pixel on replacing each pixel to the average of adjacent pixels. In the original GI tract images, filter is employed in the determination of noise without using sharpness reduction condition. The suggested method offers the effective implementation of pre=processing WCE images with the use of decorrelation stretching for attaining sharpened and enhanced image. The preprocessing of an image consists of some procedures for removing image noise, degradation of noise, correction of distortion and so on. A technique of decorrelation stretch is employed for stretching or enhancing the color variation of color image by the method that covers removal of inter-channel correlation present in pixels; thus, it is termed as decorrelation stretching.

International Journal of Environmental Sciences
ISSN: 2229-7359
Vol. 11 No. 7s, 2025
https://www.theaspd.com/ijes.php

B. Adaptive dense U-Net based segmentation

In general, U-Net is considered as a CNN that expands with few alterations in the CNN architecture. In this, the network is considered as an uncertain input image size since this is not comprising of fully connected layers. This leads to small weight size model too that could be easily scaled for having the multiple classes.

This approach of adaptive dense U-Net CNN network makes significant advancement in the identification and analysis of image.

The adaptive deep U-Net structure consists of subsequent layers like ReLU, activation, convolutional, pooling, FC (fully connected) and dense layer. This structure should be utilized for various purposes in several areas. This approach is redistributed, interpreted by making class likelihood estimation of image computation. This can be mathematically expressed as shown:

$$F = \det[N] - V\,(\text{segment}\,(N))^2 \quad (1)$$

In this, F signifies the area which are probable, N denotes the feature points that are abnormal, and $\beta_1\beta_2$ signifies the areas which are segmented and is thus mathematically shown as:

$$\det[N] = \beta_1\beta_2 \quad (2)$$

$$\text{segment}(r) = \beta_1\beta_2 \quad (3)$$

Therefore, the segmentation is concluded as:

$$F = \beta_1\beta_2 - V(\beta_1 + \beta_2)^2 \quad (4)$$

In this, V *is the empirical constant.*

The pseudocode for this algorithm is shown below:

Algorithm 1: Adaptive dense U-Net based segmentation

Input: *Segmented image* S_{m_fea}, *Data_coordinate* S_e

Output: *Segmented image* D_g

To calculate the segmented value,

For $i = 1{:}size(S_{m\_parameters}, 1)$

For $j = 1{:}size(S_{m\_features}, 1)$

$$detect(i, j) = \sqrt{(i_{m_{features}}(i, 1) - i_{m_{features}}(j - 1)) + (i_{m_{features}}(i, 1) - (i_{n_{features}}(j, 1)^2}$$

End

End

International Journal of Environmental Sciences
ISSN: 2229-7359
Vol. 11 No. 7s, 2025
https://www.theaspd.com/ijes.php

$$data\ segmented\ s_{m\_fea} = [q_{m\_fea} Distance]$$

$$Class\ label = unique(target)$$

$$K = length(class\ label)$$

$$For\ s = 1{:}k$$

$$Temp = totalclassmean(I,:)$$

$$x(I,j) = -0.3 * Temp * totalclassmean + log(i)$$

$$x(I,2{:}end) = temp$$

$$F = \beta_1 \beta_2 - V(\beta_1 + \beta_2)^2$$

$$End$$

Thus, from this, segmented part of the image is attained. Then the feature point extraction is carried based on enhanced ORB algorithm and is explained in the subsequent sections.

C. *Enhanced ORB (Oriented fast and Rotated BRIEF) algorithm-based feature point extraction*

An image feature extraction is subdivided as: detection of feature point and the description of feature point [21]. ORB is the method of image feature extraction presented by Ethan Rubble et al. in the year 2011. On comparing existing methods SIFT (scale invariant feature transform) and SURF (Speeded up robust features), the ORB speed is faster. Moreover, it is the integration of enhanced features from accelerated segment test (FAST) detection approach and an improved BRIEF (Binary robust independent elementary features) description approach. The feature point detection method, FAST is the fastest method. The base of judging whether the point is a feature for checking the point's greyscale value and another point in the circle at which the center is a point and radius is referred as R. in case, there are n continuous greyscale values that are greater or lesser than point value, then the feature point could be judged. The principle behind this is shown in figure provide below.

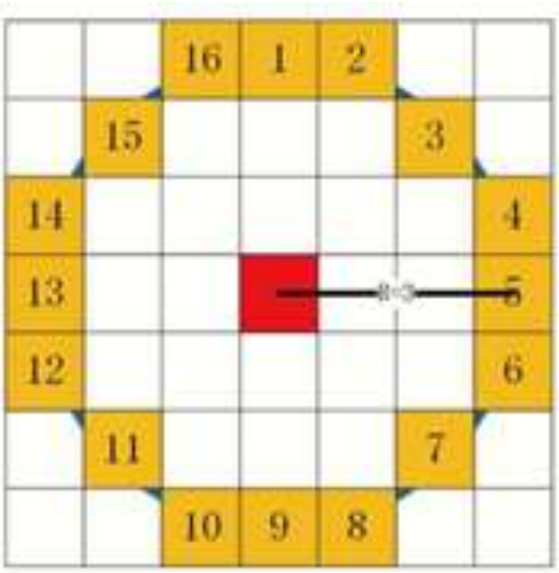

Figure 2 FAST feature point detection schematic diagram at which R takes 3 and n takes 16

An enhanced and improvised FAST is termed as oriented FAST (oFAST). The directions are thus added in oFAST on using moment technique for realizing the rotation invariance of the feature point of an image. The moment is expressed by:

$$m_{pq} = \sum_{x,y\in[-r,r]} x^p y^q I(x, y) \quad (5)$$

In this, (x, y) denotes the grey image at a point (x,y) and r denotes the feature point's neighborhood radius. The calculation of direction is expressed as:

$$\propto = arc\ tan\left(\frac{m_{01}}{m_{00}} / \frac{m_{10}}{m_{00}}\right) = arctan\left(\frac{m_{01}}{m_{10}}\right) \quad (6)$$

The method of feature description BRIEF offers a binary descriptor. This employs the function of Gaussian distribution for selecting the pairs of feature points and thus attains binary descriptor by the following equation:

$$\tau\ p; x, y := \begin{cases} 1, & if\ p(x) < p(y) \\ 0, & otherwise \end{cases} \quad (7)$$

$$f(p) := \sum_i 2^{i-1}\ \tau(p; x, y) \quad (8)$$

In this, p(x), and p(y) refers to the intensity of point x and y correspondingly, i refers to ith bit of binary descriptor.

An enhanced BRIEF is termed as rotated BRIEF. This employs a greedy search for selecting the pair of point. The desired way is to choose the pair points. The desired way is for selecting 31 × 31 neighborhood for the extracted feature point by the oriented FAST approach and an average grey scale value of the sub windows 5 × 5 is thus chosen for every neighborhood in spite of the original single point value of the pixel. by this manner, each and every neighborhood might have $L = (31 - 5)^2$ points, with a total $Q = C(L, 2)$ point pairs are formed. The greedy search is employed for this point pairs for selecting 256-point pairs further away from each other and by above 7 and 8 equations, final 256-bit feature texts are thus attained.

D. *Multi-Enhanced Deep CapsNet classification*

In the techniques that are based on neural network, a spatial patterns which are extracted at lower levels might be subsidized to high-level concept depiction. The CNN a spatially sensitive model thus paves a path for incompetence in the feature detectors replication. Moreover, the methods that are spatially sensitive are a well effectual one at the time of interference regardless of some patterns. However, they might be restricted for encoding rich structures unavoidable which are accessible in sequence.

By enhancing the efficiency of encoding the spatial patterns thus keep its ability flexible is therefore a bottleneck. Therefore, a capsule network is employed to address these concerns. Consequently, this technique should encode spatial relations intrinsically over the part thereby establishing invariant knowledge viewpoints thoroughly that generalizes to the viewpoints in an automatic manner. In this work, Multi-Enhanced Deep CapsNet classification approach is presented. The features extracted are thus passed through the operation series and therefore the hierarchical layers to attain abnormal or normal region of WCE image and is thus described as follows:

(a) N-gram Convolution layer:

The illustration attained with one sequential length and the representation of each k-dimensional token was passed initially over the convolution layer to extract and learn feature extractions from N-grams. These layers output thus feature maps over a sheafing convolution function at inner layers in the subsequent pooling which is expressed as follows:

$$f_m = U_B * k_m + b \quad (9)$$

$$f_m = p(f_m) \quad (10)$$

In this, k_m symbolizes the kernel having bias b that outputs feature map f_m through the pooling and convolution function and is signified by means of p(.). At that time, these feature maps are congregated for forming a layer of t-channel and is shown as:

$$F = [f_1, f_2, \ldots, f_t] \quad (11)$$

Hence, this layer of n-gram convolution extracts the representation of features.

(b) Bi-directional Recurrent layer:

The feature maps F attained or t-channel layer are thus directed over the bidirectional CapsNet for encoding the feature maps in a sequential manner to the hidden states thereby learning the features based sematic as shown:

$$\overrightarrow{h}_t = LSTM_{fd}(f_t, \overrightarrow{h}_{t-1}) \quad (12)$$

$$\overleftarrow{h}_t = LSTM_{bd}(f_t, \overleftarrow{h}_{t+1}) \quad (13)$$

To those each feature map, its corresponding forward and backward hidden states $\overleftarrow{h}_t$ and $\overrightarrow{h}_t$were therefore concatenated to attain single hidden state function h_t. After that, the entire matrix of hidden state is attained as shown:

$$H = [h_1, h_2, \ldots, h_t] \quad (14)$$

In this, $H \in \mathbb{R}^{t*2d}$ & d symbolizes the number of hidden units in each LSTM. Thus, in a specific phrase this layer captures a context to learn long terms dependency of WCE images.

(c) primary capsule layer:

The extracted features are thus passed through the layer of primary capsule thus fragmenting an instantiated part together with some other convolution function. In general, the layer of primary capsule uses the vectors as it is opposed to the scales to retain instantiated parameters which belongs to each feature. This is a significant part, as it depicts the intensity of activation thus maintaining some details of the instantiated input layer sections. Hence, specifically, capsuled might be termed as shorter representation of the instantiated part which are extracted through the convolutional kernels. Therefore, sliding through the H hidden state, each kernel k_m thereby outputs the sequence of capsule, $c_m \in \mathbb{R}^d$ with that of d dimension. The capsule output that comprises of channel C_m therefore belongs to the primary capsule layer. This is expressed as shown;

$$C_m = s(k_m * H + b) \quad (15)$$

In this, s denotes the function of squash which are non-linear and b denotes the weight parameter of capsule bias.

$$C = [C_1, C_2, \dots C_m] \quad (16)$$

Therefore, this layer takes the consideration of contradicting error of the traditional CNN step thereby substituting its scalar feature outcome with the vector capsules output by retaining the instantiated parameters.

(d) Connecting Capsule layer via a Dynamic routing

Usually, the capsule network therefore makes a capsule in subsequent layer by a successful routing on the agreement technique. Thus, this technique eradicates the information of location on replacing pooling function of traditional convolutional layer. However, this kind of information is extremely needed as it enhances the robustness of network on aiding clustering of features for the operation of prediction. Hence, these two consecutive layers considers $l \; and \; l + 1$, a vector $\hat{v}_{b|a}$ for the prediction is therefore computed from v_a capsule as follows:

$$\hat{v}_{b|a} = U_{ab} v_a \quad (17)$$

In this, v_a signifies the l layer of capsule. In the $l + 1$ layer, the capsule z_b is thus computed as shown:

$$z_b = \sum_a u_{ab} v_{b|a} \quad (18)$$

In this, u_{ab} denotes the coupling coefficient which are recognized by an algorithm of dynamic routing. This method therefore identifies link or connection among the b capsule of $l + 1th$ layer that validates coupling coefficient u_{ab}. The q_{ab} coupling co-efficient primary value is revised via routing over the p_{ab} agreement and is expressed as follows:

$$p_{ab} = \hat{v}_{b|a} . m_b \quad (19)$$

Here, m signifies the length of capsule. The capsule length thus signifies the likelihood that an input sample contains, the capsule object denotes the capsule activation. Henceforth, the length of capsule is thereby limited at a range of [0,1] that are having non-linear function of squashing as follows:

$$m_b = \frac{\|z_b\|^2 \quad z_b}{1+\|z_b\| \; \|z_b\|^2} \quad (20)$$

From this, the value of agreement p_{ab} is thereby added to the value for the computation of capsule value in subsequent layer and is represented as shown:

$$q_{ab} \rightarrowtail = q_{ab} + p_{ab} \quad (21)$$

The whole process from (18) to (21) is run iteratively to optimize the value of coupling coefficient and the subsequent layer of capsule. By this approach, the agreement and significance of affected or unaffected regions of WCE images were decided for the desired prediction operation.

(e) Class capsule layer with a loss:

The last layer of capsule consist of y capsules class at which each layer thus corresponds to a category of class or the label. The length of substantiated parameter length of each and evry capsule denotes the

probability of input sample which belongs to class label. Moreover, direction of each set of this substantiated parameter thereby maintains traits and aspects of the feature attributes that could be learned as the encoded vector for the input samples. To enhance the variation among various class capsule length and aids in generalization function, loss of separated margin was employed as follows:

$$L_b = R_b \max(0, e^+ - \|c_b\|^2) + \lambda(1 - R_b)\max(0, e^- - \|c_b\|^2) \quad (22)$$

Here, c_b denotes the category b capsule. e^+ & e^- denotes the top and bottom margins in a corresponding manner which forces the length over these two margins. λ denotes the weight class which are not available. Therefore, this aids in the scaling down the weight of absent class thus attaining enhanced detection.

III. PERFORMANCE ANALYSIS

The assessment of performance is carried for the proposed system and the outcomes are compared with traditional methods to prove the effectiveness of proposed method.

In table 1 the comparative assessment of proposed Adaptive dense U-Net based segmentation is carried and the attained outcomes are compared with traditional methods. This comparison is made to evaluate and prove the efficiency of proposed system. The tabulated values reveals that the proposed outcome is competent of offering better outcomes than others.

Table 1 comparative assessment for the segmentation approach

Dataset	Accuracy	Specificity	Sensitivity	Precision
Proposed (Adaptive dense U- Net)	0.9977	0.9989	0.9901	0.9972
Publicly available [23]	0.9959	0.9987	0.9849	0.9963
Grow cut segmentation [24]	0.9961	0.9965	0.9345	0.9909

The performance analysis of proposed model is thus simulated and results attained are provided in table format in table 2. The existing technique results [22] are compared with proposed outcome. The analysis proves that the proposed classifier model is effectual in offering improved outcomes on comparing traditional methodologies.

Table 2 Classifier performance comparison

Classifier	Accuracy	FNR	FPR	Precision	Recall	F- measure
Multi- Enhanced Deep CapsNet (Proposed)	0.99	0.0 27	0.029	0.985	0.972	0.963
Polynomial kernel SVM	0.954	0.0 48	0.043	0.956	0.952	0.954
SVM with EM	0.895	0.099	0.115	0.940	0.901	0.920
SVM with KNN	0.690	0.226	0.477	0.765	0.774	0.769

The proposed classifier model is thus simulated and results attained is provided in graphical form as shown in figure 3. The comparison of proposed and existing method is made in terms of accuracy, precision, recall, and F-measure. Hence, from the outcome it was apparent that the suggested model is better in offering enhanced results than existing methodologies.

International Journal of Environmental Sciences
ISSN: 2229-7359
Vol. 11 No. 7s, 2025
https://www.theaspd.com/ijes.php

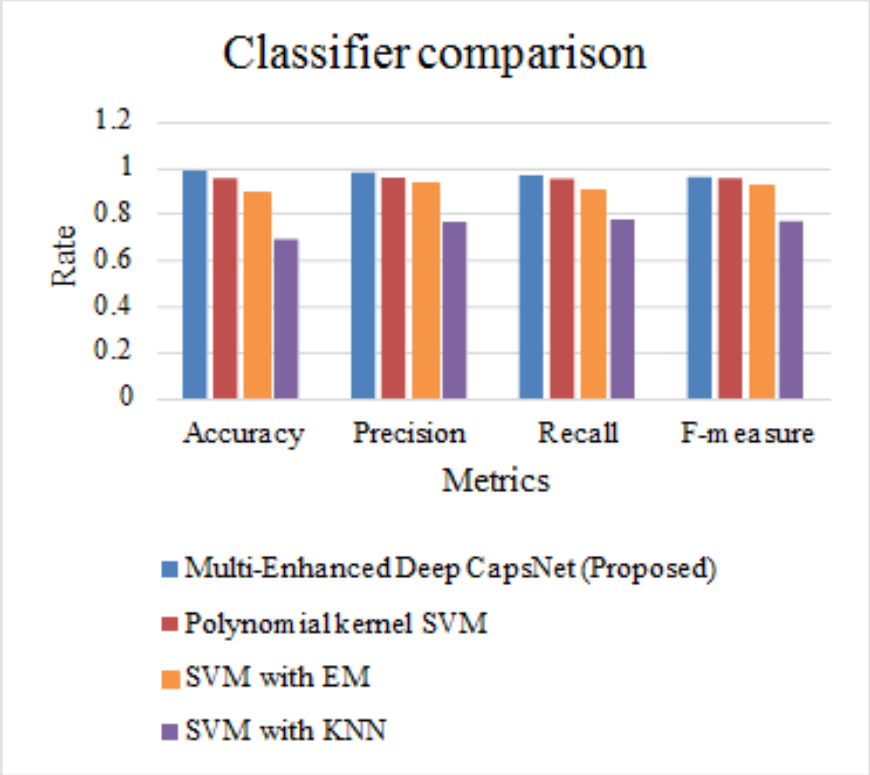

Figure 3 Classifier performance comparison

Figure 4 is the illustration of comparative assessment made for proposed existing methods in terms of FNR and FPR. The results acquired reveals that the proposed model is better in reducing errors than the existing models.

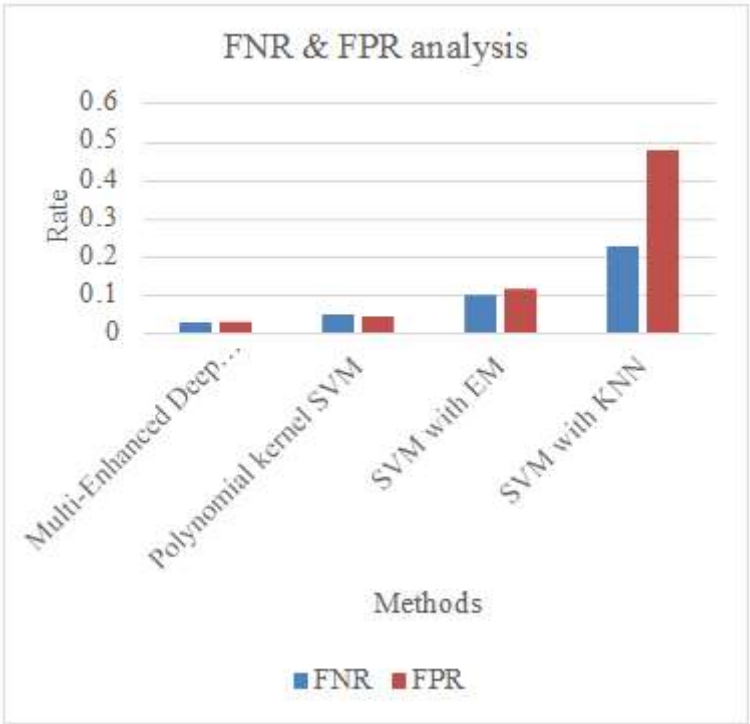

Figure 4 comparison of FNR and FPR performance

The overall detection method performance is compared and is shown in table 3. Several existing models are compared with proposed performance and the accuracy for these existing and proposed detection methods are projected. The attained outcomes shows that the proposed model is competent of offering improved accuracy on comparing traditional models.

Table 3 performance comparison of overall detection model

Classifier	Abnormality Detection Methods	Accuracy
Proposed	Adaptive dense UNet+Enhanced ORB+Multi-Enhnaced Deep CapsNet classifier	**99.97**
[25]	GMM superpixel+Color Features+Texture Features +SVM	99.88
[26]	Color features+ HSV features+ 3 SVM Classifiers	99.6
[27]	RGB Histogram + KNN	97.86
[28]	Color + Random Tree	93.4
[29]	Color histogram+KNN+SVM	98.05

The overall result comparison shows that the proposed design is much more accurate and is offering improvised outcomes than existing models. Likewise, the segmentation process and feature point extraction model employed in this work enhances the classifier performance. The error rate or proposed detection scheme seems to be lower than existing ones.

IV. CONCLUSION

This paper presents an automated deep learning-based detection and classification of bleeding region in WCE image. At first, WCE input images were pre-processed using linear filtering and distribution linearization. The segmentation approach using adaptive dense U-Net based segmentation technique was carried for the effectual segmentation of image. An enhanced ORB algorithm was employed for the feature point extraction. The process of detection and classification of the detected region as a bleeding and non-bleeding region is carried out by means of Multi-Enhanced Deep CapsNet model. The performance analysis was assessed and results were compared with existing methods in terms of sensitivity, specificity, recall, precision, accuracy, F-measure, FNR, and FPR. The acquired outcomes are compared with traditional approaches to validate the effectiveness of proposed approach to that of existing models. It was evident from the attained results that the proposed model shows improvement in accuracy rate, sensitivity, specificity, precision, recall, F- measure thereby providing reduced error rate. Henceforth, the suggested technique was considered as an effective mechanism in offering improvised performance.

REFERENCES

[1] Patel, A., Rani, K., Kumar, S., Figueiredo, I. N., & Figueiredo, P. N. (2021). Automated bleeding detection in wireless capsule endoscopy images based on sparse coding. *Multimedia Tools and Applications*, *80*, 30353- 30366.

[2] Guo, X., & Yuan, Y. (2020). Semi-supervised WCE image classification with adaptive aggregated attention. *Medical Image Analysis*, *64*, 101733.

[3] Mandal, S., Adhikari, M., Banerjee, S., & Chaudhuri, S. S. (2019, May). Novel Adaptive Statistical Method-CNN Synergism Based Two-Step WCE Image Segmentation. In *2019 International Conference on Intelligent Computing and Control Systems (ICCS)* (pp. 1024-1029). IEEE.

[4] Xing, X., Yuan, Y., & Meng, M. Q. H. (2020). Zoom in lesions for better diagnosis: Attention guided deformation network for wce image classification. *IEEE Transactions on Medical Imaging*, *39*(12), 4047-4059.

[5] Muruganantham, P., & Balakrishnan, S. M. (2021). A survey on deep learning models for wireless capsule endoscopy image analysis. *International Journal of Cognitive Computing in Engineering*, *2*, 83-92.

[6] Latha, R. S., Sreekanth, G. R., Murugeasan, G., Aruna, S., Inbaraj, B., Kanivel, S., & Karthikeyan, S. (2021). Deep Learning based Automatic Detection of Intestinal Hemorrhage Using Wireless Capsule Endoscopy Images. *NVEO-NATURAL VOLATILES & ESSENTIAL OILS Journal| NVEO*, 92-103.

[7] Xiao, Z., Lu, J., Wang, X., Li, N., Wang, Y., & Zhao, N. (2022). WCE-DCGAN: A data augmentation method based on wireless capsule endoscopy images for gastrointestinal disease detection. *IET Image Processing*.

[8] Khan, M. A., Kadry, S., Alhaisoni, M., Nam, Y., Zhang, Y., Rajinikanth, V., & Sarfraz, M. S. J. I. A. (2020). Computer-aided gastrointestinal diseases analysis from wireless capsule endoscopy: a framework of best features selection. *8*, 132850-132859.

[9] Alam, M. W., Vedaei, S. S., & Wahid, K. A. J. C. (2020). A fluorescence-based wireless capsule endoscopy system for detecting colorectal cancer. 12(4), 890.

[10] Gu, Y., Xie, X., Li, G., Sun, T., & Wang, Z. (2012). Two- stage wireless capsule image compression with low complexity and high quality. Electronics letters, 48(25), 1588-1589.

[11] Aghanouri, M., Ghaffari, A., Serej, N. D. J. J. o. I., & Systems, R. (2019). Image based high-level control system design for steering and controlling of an active capsule endoscope. 94(1), 115-134.

[12] Du, W., Rao, N., Liu, D., Jiang, H., Luo, C., Li, Z., . . . Zeng, B. (2019). Review on the applications of deep learning in the analysis of gastrointestinal endoscopy images. Ieee Access, 7, 142053-142069.

[13] Aoki, T., Yamada, A., Aoyama, K., Saito, H., Tsuboi, A., Nakada, A., . . . Ishihara, S. J. G. e. (2019). Automatic detection of erosions and ulcerations in wireless capsule endoscopy images based on a deep convolutional neural network. 89(2), 357-363. e352.

[14] Jain, S., Seal, A., Ojha, A., Krejcar, O., Bureš, J., Tachecí, I., . . . medicine. (2020). Detection of abnormality in wireless capsule endoscopy images using fractal features. 127, 104094.

[15] Sainju, S., Bui, F. M., & Wahid, K. A. (2014). Automated bleeding detection in capsule endoscopy videos using statistical features and region growing. *Journal of medical systems, 38*(4), 1-11.

[16] Xing, X., Jia, X., & Meng, M. Q.-H. (2018). Bleeding detection in wireless capsule endoscopy image video using superpixel-color histogram and a subspace KNN classifier. Paper presented at the 2018 40th Annual International Conference of the IEEE Engineering in Medicine and Biology Society (EMBC).

[17] Rahim, T., Usman, M. A., & Shin, S. Y. (2020). A survey on contemporary computer-aided tumor, polyp, and ulcer detection methods in wireless capsule endoscopy imaging. Computerized Medical Imaging and Graphics, 101767.

[18] Chaibou, M. S., Conze, P.-H., Kalti, K., Solaiman, B., & Mahjoub, M. A. (2017). Adaptive strategy for superpixel-based region-growing image segmentation. Journal of Electronic Imaging, 26(6), 061605.

[19] Charfi, S., El Ansari, M., & Balasingham, I. J. I. I. P. (2019). Computer-aided diagnosis system for ulcer detection in wireless capsule endoscopy images. 13(6), 1023-1030.

[20] Mo, X., Tao, K., Wang, Q., & Wang, G. (2018). An efficient approach for polyps detection in endoscopic videos based on faster R-CNN. Paper presented at the 2018 24th international conference on pattern recognition (ICPR).

[21] Tian, X., Zhou, G., & Xu, M. (2020). Image copy-move forgery detection algorithm based on ORB and novel similarity metric. *IET Image Processing*, *14*(10), 2092- 2100.

[22] Amiri, Z., Hassanpour, H., & Beghdadi, A. J. J. o. H. E. (2021). A Computer-Aided Method for Digestive System Abnormality Detection in WCE Images. 2021.

[23] Floch, M. H. (2008). Capsule Endoscopy. In: LWW.

[24] Deeba, F., Bui, F. M., & Wahid, K. A. (2016). Automated growcut for segmentation of endoscopic images. Paper presented at the 2016 International Joint Conference on Neural Networks (IJCNN).

[25] Rathnamala, S., Jenicka, S. J. M., Engineering, B., & Computing. (2021). Automated bleeding detection in wireless capsule endoscopy images based on color feature extraction from Gaussian mixture model superpixels. 59(4), 969-987.

[26] Deeba, F., Islam, M., Bui, F. M., Wahid, K. A. J. B. S. P., & Control. (2018). Performance assessment of a bleeding detection algorithm for endoscopic video based on classifier fusion method and exhaustive feature selection. 40, 415-424.

[27] Kundu, A. K., Fattah, S. A., & Rizve, M. N. J. J. o. h. e. (2018). An automatic bleeding frame and region detection scheme for wireless capsule endoscopy videos based on interplane intensity variation profile in normalized RGB color space. 2018.

[28] Pogorelov, K., Suman, S., Azmadi Hussin, F., Saeed Malik, A., Ostroukhova, O., Riegler, M., . . . Goh, K. L. J. J. o. a. c. m. p. (2019). Bleeding detection in wireless capsule endoscopy videos—color versus texture features. 20(8), 141-154.

[29] Yuan, Y., Li, B., Meng, M. Q.-H. J. I. j. o. b., & informatics, h. (2015). Bleeding frame and region detection in the wireless capsule endoscopy video. 20(2), 624-630.